Isospin structure of $J^\pi = 1^+$ states in ^{58}Ni and ^{58}Cu studied by ^{58}Ni(p, p') and ^{58}Ni(^{3}He,t)^{58}Cu measurements

H. Fujita,[1,*] Y. Fujita,[1] T. Adachi,[1,†] A. D. Bacher,[2] G. P. A. Berg,[3,‡] T. Black,[2] E. Caurier,[4] C. C. Foster,[2] H. Fujimura,[3,§] K. Hara,[3,‖] K. Harada,[1] K. Hatanaka,[3] J. Jänecke,[5] J. Kamiya,[6,¶] Y. Kanzaki,[1] K. Katori,[1] T. Kawabata,[3,**] K. Langanke,[6,††] G. Martínez-Pinedo,[6,††] T. Noro,[3,‡‡] D. A. Roberts,[5] H. Sakaguchi,[7,§§] Y. Shimbara,[1,‖‖] T. Shinada,[1] E. J. Stephenson,[2] H. Ueno,[1,¶¶] T. Yamanaka,[3] M. Yoshifuku,[1] and M. Yosoi[7,†]

[1]*Department of Physics, Osaka University, Toyonaka, Osaka 560-0043, Japan*

[2]*Indiana University Cyclotron Facility (IUCF), Bloomington, Indiana 47408, USA*

[3]*Research Center for Nuclear Physics (RCNP), Osaka University, Ibaraki, Osaka 567-0047, Japan*

[4]*Institut de Recherches Subatomiques (IN2P3-CNRS/Université Louis Pasteur), F-67037 Strasbourg Cedex 2, France*

[5]*Physics Department, University of Michigan, Ann Arbor, Michigan 48109, USA*

[6]*Institute of Physics and Astronomy, University of Aarhus, DK-8000 Aarhus C, Denmark*

[7]*Department of Physics, Kyoto University, Sakyo, Kyoto 606-8502, Japan*

(Received 31 March 2006; published 21 March 2007)

Isospin is a good quantum number under the assumption that the nuclear interaction is charge independent. An analogous structure of excited states is expected for nuclei with the same mass number A but with different z components T_z of the isospin T, where $T_z = (N - Z)/2$. The analogous structure has been studied for the isobaric nuclei ^{58}Ni and ^{58}Cu by comparing the transitions from the ^{58}Ni ground state (initial isospin $T_i = 1$ and $J^\pi = 0^+$) to the $M1$ and the Gamow-Teller (GT) states ($J^\pi = 1^+$) in ^{58}Ni and ^{58}Cu, respectively. For this purpose, proton inelastic scattering (p, p') at $E_p = 160$ MeV and the charge-exchange (^{3}He,t) reaction at 140 MeV/nucleon were both measured at 0°, exciting final states with isospin $T_f = 1$ and 2 and $T_f = 0$, 1, and 2, respectively. High energy and scattering-angle resolutions were achieved by applying complete beam matching techniques. On the basis of the correspondence between excitation energies and transition strengths, isospin values $T_f = 1$ and 2 of analog GT and $M1$ states were identified. The distribution of $T_f = 2$ states was also compared with results of ^{58}Ni(d,^{2}He), ^{58}Ni(t,^{3}He), and ^{58}Ni(n, p) experiments, in which only $T_f = 2$ states are excited. The obtained GT strength distribution is compared with the results of shell-model calculations.

DOI: 10.1103/PhysRevC.75.034310 PACS number(s): 25.40.Ep, 24.30.Cz, 25.55.Kr, 27.40.+z

I. INTRODUCTION

Assuming that isospin T is a good quantum number, isospin multiplet states are found in nuclei with the same mass number A (called isobars) but with different z components of isospin defined by $T_z = (N - Z)/2$. These multiplet states are called isobaric analog states, or simply analog states. Various transitions connecting corresponding analog states are called analogous transitions. Good examples are the excitations to the Gamow-Teller (GT) and $M1$ states resulting from a charge-exchange (CE) reaction and an inelastic (IE) scattering starting, respectively, from the same ground state (g.s.) of a nucleus.

The GT transitions are caused by a simple $\sigma\tau$ operator and are characterized by $\Delta L = 0$ and spin-isospin flip. Starting from the $J^\pi = 0^+$ g.s. of an even-even nucleus, GT transitions excite $J^\pi = 1^+$ GT states. The reduced GT transition strength B(GT) is an important physical quantity for the understanding of nuclear structure [1,2] as well as for the calculation of astrophysical processes [3,4]. The transition strengths B(GT) can be determined directly from GT β decay. These studies, however, are limited to energetically allowed low excitation energies. CE reactions such as (p, n) or (^{3}He,t) performed at intermediate energies ($\geqslant$100 MeV/nucleon) can be used to map the GT strengths over a wider range of excitation energies [5]. For this purpose, one relies upon the approximate proportionality between the $L = 0$ components of the reaction cross sections at 0° scattering angle and the B(GT) values.

*Present address: School of Physics, University of the Witwatersrand, Johannesburg 2050, South Africa; Also at: iThemba LABS, Somerset West 7129, South Africa; E-mail address: hfujita@tlabs.ac.za

†Present address: Research Center for Nuclear Physics (RCNP), Osaka University, Ibaraki, Osaka 567-0047, Japan.

‡Present address: Department of Physics, University of Notre Dame, Indiana 46556, USA.

§Present address: Department of Physics, Kyoto University, Sakyo, Kyoto 606-8502, Japan.

‖Present address: KEK, High Energy Accelerator Research Organization, Tsukuba, Ibaraki 305-0801, Japan.

¶Present address: Japan Atomic Energy Agency (JAEA), Tokai, Ibaraki 319-1195, Japan.

**Present address: CNS, University of Tokyo, RIKEN campus, Wako, Saitama 351-0198, Japan.

††Present address: GSI, 64291 Darmstadt, Germany.

‡‡Present address: Department of Physics, Kyushu University, Higashi, Fukuoka 812-8581, Japan.

§§Present address: Faculty of Engineering, University of Miyazaki, Miyazaki 889-2192, Japan.

‖‖Present address: NSCL, Michigan State University, East Lansing, Michigan 48824, USA.

¶¶Present address: RIKEN, Wako, Saitama 351-0198, Japan.

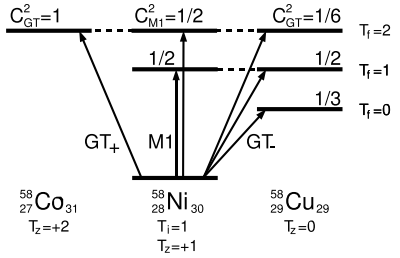

FIG. 1. Schematic view of isospin structure for $A = 58$ nuclei, showing allowed T_f values and Clebsch-Gordan coefficients for corresponding GT_+, $M1$, and GT_- transitions from the $T_i = 1$ target nucleus ^{58}Ni.

$M1$ γ decay is a result of $\Delta J = 1$ without a parity change. Similarly, excitations via the electromagnetic interaction are referred to as $M1$, and the excited states are called $M1$ states. Thus, starting from a $J^\pi = 0^+$ g.s., $M1$ states have $J^\pi = 1^+$. Proton IE scattering at intermediate incident energies and at 0° is suited for the study of transitions to $M1$ states.

The simplest isospin symmetry structure of excited states, i.e., the analogous structure in T_z, is expected for the odd-mass mirror nuclei with $T_z = \pm 1/2$. The isospin symmetry structure of excited states in $T_z = \pm 1/2$ nuclei has been studied for *sd*-shell nuclei. Contributions of the isovector (IV) orbital term and the isoscalar (IS) term have been discussed in a transition-by-transition comparison of the strengths in analogous excitations to GT and $M1$ states in Refs. [6–9].

In a so-called $T = 1$ system shown in Fig. 1, the isospin structure becomes more complicated and a variety of analogous transitions are expected. In (p, n)-type CE and in IE scattering reactions, starting from the g.s. of a $N = Z + 2$ nucleus with isospin $T_i = 1$, transitions to GT and $M1$ states in nuclei with $T_z = 0$ and $+1$, respectively, can be studied. The allowed isospin values T_f of the final GT and $M1$ states starting from ^{58}Ni are shown in Fig. 1.

The nucleus ^{58}Ni is the heaviest, stable $T_z = +1$ target. The decomposition of GT strength for three different isospin values can be found in Ref. [10]. There, the authors discuss the isospin decomposition by comparing the GT strength distribution from a ^{58}Ni(^{3}He,t) measurement at 0° and the $M1$ strengths from a ^{58}Ni(e, e') measurement [11]. However, the energy resolution ΔE of 140 keV [full width at half maximum (FWHM)] in the (^{3}He,t) reaction was not sufficient to make a detailed comparison with the $M1$ distribution studied with $\Delta E =$ 30 keV. A better resolution was needed in the (^{3}He,t) reaction.

A higher energy-resolution ^{58}Ni(^{3}He,t) experiment was performed to study the structure of the ^{58}Cu nucleus [12]. Here, the GT strength distribution in ^{58}Cu was studied up to the excitation energy E_x of 8.3 MeV with an energy resolution of 50 keV (FWHM). As will be described, it is known that only $T_f = 0$ and 1 GT states exist in this region. The GT strength distribution was compared with the $M1$ strengths from a nuclear resonance fluorescence (NRF) measurement on ^{58}Ni [13]. Candidates for analog $M1$ states for a few GT states were identified above 7 MeV, suggesting that these GT states have $T_f = 1$. By the ^{58}Ni(^{3}He,tp) and ^{58}Ni(^{3}He,$t\gamma$) coincidence measurements, the branching ratios for proton and γ decay from the GT and the spin dipole resonances were studied [14]. The result suggested that $T = 1$ and 2 GT states with an $f_{7/2}$ neutron-hole have a coupling to two particle-two hole (2p-2h) configurations.

In this paper, we present the experimental results of ^{58}Ni(^{3}He,t) and ^{58}Ni(p, p') reactions performed at 0° and intermediate incident energies of 140 MeV/nucleon and 160 MeV, respectively. The energy resolution was 35 keV (FWHM) in both measurements. Because of the high energy resolution in the (^{3}He,t) reaction, the GT giant resonance, observed as a bumplike structure at $E_x \approx 10$ MeV in the ^{58}Ni(p, n) reaction [15], was resolved into discrete states. Transitions with angular momentum transfer $\Delta L = 0$ were identified thanks to the good scattering-angle resolution. By comparing the (^{3}He,t) and the (p, p') results, we discuss the isospin symmetry structure of highly excited $M1$ and GT states up to $E_x = 13$ MeV. The value of the isospin T_f is assigned for each pair of $M1$ and GT states by comparing the transition strengths. We compare our data also with the results from ^{58}Ni(d,^{2}He) [16], ^{58}Ni(t,^{3}He) [17], and ^{58}Ni(n, p) [18] reactions, in which only states with $T_f = 2$ are excited. It is expected that these comparisons will reveal the isospin structure in the $A = 58$ system. The GT strength distribution is compared with the shell-model calculations.

II. CHARACTERISTICS OF 1^+ TRANSITIONS

A. Reduced transition strengths

The reduced GT transition strength B(GT) is a fundamental quantity. Following the convention of Edmonds [19], B(GT) can be expressed [8] by the equation

$$B(\mathrm{GT}) = \frac{1}{2}\,\frac{1}{2J_i+1}\,\frac{C_{\mathrm{GT}}^2}{2T_f+1}\,[M_{\mathrm{GT}}(\sigma\tau)]^2, \qquad (1)$$

where C_{GT} is the isospin Clebsch-Gordan (CG) coefficient and $M_{\mathrm{GT}}(\sigma\tau)$ is a GT matrix element that is reduced in both spin and isospin. The squared values of C_{GT} to different T_f states are shown in Fig. 1.

Hadron CE reactions such as (p, n), especially those performed at incident energies above 100 MeV/nucleon and small scattering angles close to or including 0° (momentum transfer $q \approx 0$), have been used as a means to map GT strengths over a wide range of excitation energies. Under these conditions, GT transitions are generally prominent and $\Delta L \neq 0$ transitions are strongly suppressed [1,20]. A good proportionality between the (p, n) cross sections at 0° and B(GT) values was empirically established [5],

$$\frac{d\sigma^{\mathrm{CE}}}{d\Omega}(0^\circ) \cong K^{\mathrm{CE}} N_{\sigma\tau}^{\mathrm{CE}} |J_{\sigma\tau}(q=0)|^2 B(\mathrm{GT}) = \hat{\sigma}_{\mathrm{GT}} B(\mathrm{GT}), \qquad (2)$$

where $J_{\sigma\tau}(q = 0)$ is the volume integral of the effective interaction $V_{\sigma\tau}$ at zero momentum transfer $q = 0$, and K^{CE} and $N_{\sigma\tau}^{\mathrm{CE}}$ are kinematic and distortion factors, respectively. The value $\hat{\sigma}_{\mathrm{GT}}$ is the so-called GT unit cross section. For the determination of B(GT) values using Eq. (2), a standard value

is needed. In principle, standard values should come from a β-decay measurement for allowed GT transitions.

It has been found that the approximate proportionality given by Eq. (2) is usually valid in (^{3}He,t) reactions at 140 MeV/nucleon. However, an exceptional case has been found recently for transitions with $j_< \rightarrow j_<$ configurations [21,22]. In the (^{3}He,t) reaction, an uncertainty of 30–50% has been found for a few low-lying states in $A = 37$ and 41 nuclei in which the $d_{3/2}$ configuration is largely involved. Similar findings were also reported in (p, n) reactions [23]. In addition, depending on the configurations of GT states, the contribution of the tensor-τ type of effective interaction term can be large. It is usually believed that this contribution is small at small momentum transfer [1,20], as mentioned, but if the contribution cannot be neglected, the proportionality relationship would not be valid.

The $M1$ states are prominently excited in proton IE scattering at 0° and at incident energies larger than 100 MeV/nucleon. This is again due to the dominance of the $V_{\sigma\tau}$ component of the effective interaction [1,20]. If contributions from minor isoscalar and tensor-type operator and exchange terms are small, a proportionality similar to Eq. (2) is expected also in the (p, p') reaction. The contributions of these terms in both CE and proton IE scattering will be estimated by the distorted-wave Born approximation (DWBA) calculations in Secs. III B and IV B. The reduced transition strength denoted by $B_{\rm IE}$(GT) in this paper is given by

$$\frac{d\sigma^{\rm IE}}{d\Omega}(0^\circ) \cong K^{\rm IE} N^{\rm IE}_{\sigma\tau} |J_{\sigma\tau}(q=0)|^2 B_{\rm IE}({\rm GT}) = \hat{\sigma}^{\rm IE}_{\rm GT} B_{\rm IE}({\rm GT}), \quad (3)$$

where $\hat{\sigma}^{\rm IE}_{\rm GT}$ is the unit cross section for the $B_{\rm IE}$(GT) value. The strength $B_{\rm IE}$(GT) is defined by the equation

$$B_{\rm IE}({\rm GT}) = \frac{1}{2}\,\frac{1}{2J_i+1}\,\frac{C^2_{M1}}{2T_f+1}\,[M_{M1}(\sigma\tau)]^2. \quad (4)$$

The reduced $M1$ transition strength $B(M1)$ is also a fundamental quantity. It can be derived from measurements of γ decay, NRF, and (e, e') reactions, with details discussed in Ref. [8]. Since the $\sigma\tau$ term is dominant in both $B(M1)$ and $B_{\rm IE}$(GT), approximate proportionality is expected between the 0° cross sections of proton IE scattering and $B(M1)$ values.

B. Ratio of analogous strengths in hadron reactions

The $T_f = 1$ and 2 states are excited in both (^{3}He,t) and (p, p') reactions on $T_i = 1$ target nuclei. Because of the different isospin Clebsch-Gordan coefficients, the ratios of strengths exciting analog states with $T_f = 1$ and 2 states, however, are different.

Equations (1) and (2), and Eqs. (3) and (4), show that cross sections of GT ($\sigma\tau$-type) transitions measured in (^{3}He,t) and (p, p') reactions at 0° are proportional to the square of the isospin CG coefficients $C^2_{\rm GT}$ and C^2_{M1}, respectively. Allowed final isospin values T_f of GT and $M1$ states and the $C^2_{\rm GT}$ and C^2_{M1} values of the transitions to these states from the g.s. of ^{58}Ni are summarized in Fig. 1. It should be noted that the values of $C^2_{\rm GT}$ and C^2_{M1} are both 1/2 for the analogous transitions to the $T_f = 1$ $M1$ and GT states. On the other hand, these values are 1/2 and 1/6 for those transitions to the $T_f = 2$ $M1$ and GT states. Combining Eqs. (1) and (4), we see that the ratio $R_{\rm GT}$ for analogous transitions defined by the following equation has the values

$$R_{\rm GT} = \frac{1}{R_{\rm MEC}}\,\frac{B_{\rm IE}({\rm GT})}{B({\rm GT}_-)} = \begin{cases} 3 & \text{if} \quad T_f = 2, \\ 1 & \text{if} \quad T_f = 1, \end{cases} \quad (5)$$

where $R_{\rm MEC}$ is a ratio representing the different contribution of the so-called meson exchange currents (MEC) in the $\sigma\tau$ term of the $M1$ and GT matrix elements because of their τ_0 and τ_- natures, and is defined by

$$R_{\rm MEC} = \frac{[M_{M1}(\sigma\tau)]^2}{[M_{\rm GT}(\sigma\tau)]^2}. \quad (6)$$

The most probable value $R_{\rm MEC} = 1.25$ has been deduced for nuclei in the middle of the *sd* shell, although values in the range of 1.15–1.5 have been suggested in different experiments [8]. Therefore, the ratios of cross sections of the analogous transitions to the $M1$ and GT states with $T_f = 1$ and 2 differ by a factor of 3. By experimentally examining this ratio $R_{\rm GT}$ for each pair of analogous excitations to GT and $M1$ states, the isospin T_f can be identified by using the T_f dependence of the $R_{\rm GT}$ value. The $T_f = 0$ GT states can be identified from the nonexistence of the corresponding $M1$ states. Isospin identification using the empirically obtained $R_{\rm GT}$ values will be discussed in Sec. V A.

III. PROTON INELASTIC SCATTERING

A. Experiment

The ^{58}Ni(p, p') experiment was performed at the Indiana University Cyclotron Facility (IUCF). The 160 MeV proton beam from the cyclotron was used to bombard an enriched ^{58}Ni target of areal density 2.5 mg/cm^2.

Inelastically scattered protons were momentum analyzed by the quadrupole-dipole-dipole (QDD)-type K600 magnetic spectrometer [24]. Two sets of multiwire drift chambers were installed in the focal plane of the spectrometer. Two wire planes were used to measure horizontal positions and angles, while one wire plane was used for the vertical-position measurement. Downstream from these chambers, two ΔE-type plastic scintillators were installed for particle identification and for generating fast timing signals. To achieve the best possible energy resolution, the dispersion of the beam was matched to that of the spectrometer [24–27]. Corrections for kinematic effects were made by software. The vertical component of the scattering angle ϕ was determined by using the vertical position of particles in the focal plane with the K600 magnetic spectrometer set in a point-to-parallel transport mode [28]. To reconstruct scattering angles from focal plane parameters, a multihole calibration aperture was used at the entrance of the spectrometer.

For inelastic scattering measurements at 0°, the "transmission mode" of the K600 magnetic spectrometer, in which the incoming beam passes through the spectrometer together with inelastically scattered particles, was applied. The beam was

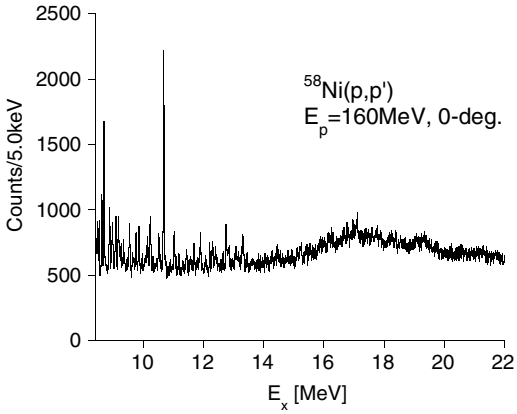

FIG. 2. Excitation energy spectrum of the ^{58}Ni(p, p') measurement between 8 and 22 MeV. Energy resolution is 35 keV. GDR bump is observed above $E_x = 16$ MeV. Events are shown for scattering angles of $\sqrt{\theta^2 + \phi^2} \leqslant 1.0^\circ$.

stopped downstream from the spectrometer in a Faraday cup placed at the higher momentum end of the focal plane. The high-dispersive focal plane of the K600 magnetic spectrometer was used to make it possible to observe an excitation energy as low as possible. Excitation energies above 8 MeV could be measured with this configuration. To eliminate events from particles scattered from the target frame, the low-momentum side of the frame was removed.

An active collimator with a circular 36 mrad opening angle was used to define the solid angle of the spectrometer and to prevent background from slit-edge scattering. Since this active collimator was slightly smaller than the opening angle of the spectrometer, it enabled a veto to be applied to remove those events that originated from slit-edge scattered protons or the beam halo from the spectrum.

The cyclotron and the beamline were carefully tuned to ensure single-turn extraction and to minimize the beam halo, essential for the reduction of background. At a beam current of about 1 nA, the beam-related background was about 100 events per second. Online fine tuning of the complete beamline with the detector system running and an empty target frame installed was essential to reduce the background.

Near 0°, the scattering angle Θ is defined by $\sqrt{\theta^2 + \phi^2}$, where θ and ϕ represent horizontal and vertical components of scattering angles, respectively. In Fig. 2, an energy spectrum between 8 and 22 MeV for scattering angles $0^\circ \leqslant \Theta \leqslant 1^\circ$ is shown. A bump-like structure is observed above $E_x = 16$ MeV, although the counting statistics are not very high. The excitation energy of this bump is in agreement with that of the giant dipole resonance (GDR) reported in Ref. [29]. It is highly probable that the GDR can be Coulomb excited at an intermediate incident energy, suggesting that a high energy-resolution (p, p') experiment at 0° could be a good tool for the study of fine structure, if any, of the GDR. An energy resolution of 35 keV ($\Delta E/E = 2.2 \times 10^{-4}$) was achieved. Discrete states were found up to about 13.5 MeV excitation energy. An energy spectrum of this region is shown in Fig. 3. Here, candidates for $M1$ states identified in the analysis described below are indicated by vertical arrows.

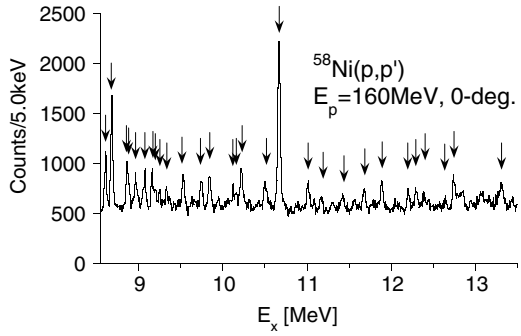

FIG. 3. Excitation energy spectrum between 8.55 and 13.5 MeV for ^{58}Ni(p, p'). Candidates of $M1$ states are indicated by vertical arrows.

B. Data analysis

In addition to the measurement for a ^{58}Ni target, data were also taken for $^{\text{nat}}$C, ^{24}Mg, and ^{54}Fe targets to calibrate excitation energies. At regular intervals, data for the carbon target were taken to monitor drifts of the magnetic fields of the spectrometer and the beam energy during the entire experiment, which lasted over one week. For this purpose, we monitored the position of the well-isolated, strong 15.11 MeV state in ^{12}C. The excitation energies of the states [30] used in the calibration were reproduced within 10 keV. In the range from 8.2 up to 15.1 MeV, excitation energies were obtained by interpolation.

For the determination of cross sections, peak intensities were derived by peak deconvolution software. The peak shape of the well-isolated 10.71 MeV state in ^{24}Mg was used as a reference. No obvious differences of peak shape and width were found for the peaks throughout the complete ^{58}Ni excitation energy spectrum.

Background in 0° scattering spectra can have a variety of physical and instrumental origins. The background was, therefore, estimated by a smooth empirical function. The errors of the extracted strengths were determined by taking into account the squared sum of the estimated background, the statistical errors, and the peak deconvolution errors.

The angle 0° was verified using the angular distributions of $L = 0$ states, which have the maximum at $\Theta = 0^\circ$. Angular distributions of observed states were obtained within the 2° acceptance of the K600 magnetic spectrometer placed at 0°.

Several electric dipole ($E1$) states reported by Bauwens *et al.* [13] were seen in the (p, p') spectrum, which are excited via the Coulomb interaction. A distorted-wave Born approximation (DWBA) calculation using the code DWBA98 [31] suggests that both angular distributions of transitions to $M1$ and Coulomb-excited $E1$ states have a maximum at 0°. These transitions, therefore, could not be well distinguished by the empirical angular distributions. In addition to these discrete $E1$ states, the GDR was observed as a broad bumplike structure of many overlapping peaks above 16 MeV in the (p, p') spectrum (see Fig. 2).

The E_x and q dependence of the unit cross section $\hat{\sigma}_{\text{GT}}^{\text{IE}}$ at 0° defined in Eq. (3) was estimated by a DWBA calculation using optical potential parameters for ^{58}Ni from Ref. [32]. Two-body interaction strengths were taken from Ref. [20].

The shell-model configurations of $(f_{5/2}, f_{7/2}^{-1})$ and $(p_{1/2}, p_{3/2}^{-1})$ were considered. It was found that $\hat{\sigma}_{\rm GT}^{\rm IE}$ gradually decreases with increasing excitation energy. At 8 and 14 MeV, it was about 90% and 80%, respectively, of its value at $E_x = 0$ MeV, irrespective of the configurations. The corrected cross sections were used in the calculation of $R_{\rm GT}$ values. As written in Sec. II, the proportionalities between the cross sections at 0° and the B(GT) and $B_{\rm IE}$(GT) values can be affected by the contributions of tensor and IS terms of the interaction, which makes the empirical $R_{\rm GT}$ ratio ambiguous. The exchange term may also influence the proportionalities. By DWBA calculations, the contributions of these terms in the (p, p') reaction were estimated to be less than 25% in total, due mainly to the IS interaction.

C. Comparison with literature values

Proton inelastic scattering on ^{58}Ni at small scattering angles down to 4° was measured using a 200 MeV beam at Orsay [33]. Excitation energies of several discrete states were reported. All corresponding states were found in the present (p, p') spectra at 9.835, 10.211, 10.492, 10.664, 11.003, and 11.883 MeV, as shown in Table I. Both results are in good agreement. With our improved resolution, however, we could observe many more excited states.

As discussed in Sec. II A, quasiproportionality is expected between (p, p') cross sections at 0° and $B(M1)$ values from electromagnetic excitations, since the isovector spin $(\sigma\tau)$ term dominates in both transitions.

In ^{58}Ni, $M1$ states have been identified up to 15 and 10 MeV excitation from the (e, e') measurement at Darmstadt [11] and the NRF measurement at Gent [13], respectively. In Fig. 4 and Table I, the cross sections of states observed in our (p, p') spectrum at 0° are shown together with the reported $B(M1)$ values of states observed in the (e, e') and NRF measurements. These states show good agreement in their excitation energies. However, several states, such as those at 8.238 and 8.517 MeV, were more strongly excited in the (e, e') experiment. These states and those at 8.880 and 9.526 MeV were assigned to be $E1$ as the result of the NRF measurement. We assume these states to be $E1$ in the following analysis.

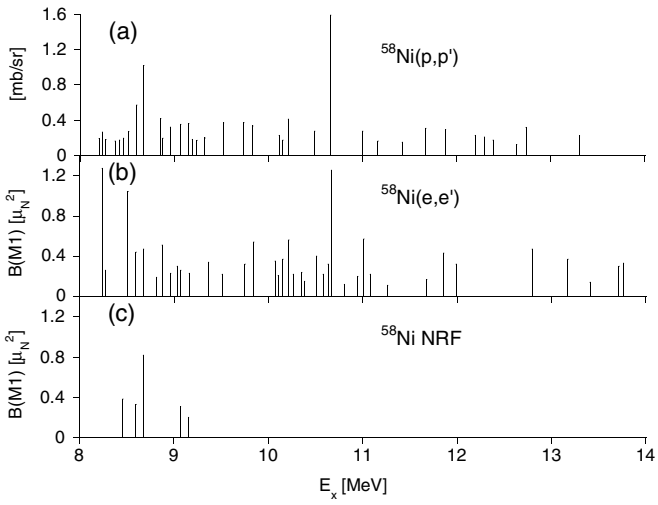

FIG. 4. Strength distributions of $J^\pi = 1^+$ states observed in ^{58}Ni for (a) (p, p') scattering, (b) (e, e') scattering [11], and (c) NRF [13] measurements.

In the NRF measurement, the excited states at 8.461, 8.602, 8.677, 9.071, and 9.156 MeV were assigned to be $M1$, as shown in Table I and Fig. 4(c). Corresponding states were also observed in the (p, p') spectrum. They are of $T_f = 1$ nature, as will be discussed later. Although these $T_f = 1$ states can have IS contributions, the relative strengths are consistent with our (p, p') measurement, suggesting the dominance of IV contributions and good proportionalities between (p, p') cross sections and the $B_{\rm IE}$(GT) values.

IV. CHARGE-EXCHANGE REACTION

A. Experiment

The ^{58}Ni(^{3}He,t) experiment at 0° was performed at the Research Center for Nuclear Physics (RCNP), Osaka University, by using a 140 MeV/nucleon ^{3}He beam from the RCNP ring cyclotron [34]. Here also the *lateral dispersion matching* technique was applied [27] in order to achieve high energy resolution. In addition, to optimize angular resolution, the *angular dispersion matching technique* [27] was applied. The WS course beamline [35] was used to transport a roughly 5 nA current of a ^{3}He^{2+} beam onto the target. As diagnostics of the matching and focusing conditions [27], the *faint beam method* [26] was used. A thin ^{58}Ni target of 1.5 mg/cm^2 areal density was used to reduce the energy broadening effect. It is estimated that the effect is about 20 keV as a result of the difference of ^{3}He and triton energy losses.

Scattered particles were momentum analyzed by the Grand Raiden magnetic spectrometer [36]. The horizontal and vertical angular acceptances were set to 40 and 80 mr, respectively, by a rectangular aperture installed at the entrance of the spectrometer. The ^{3}He^{2+} beam, with about half the magnetic rigidity $B\rho$ of the tritons, had a much smaller bending radius in the spectrometer and was stopped in a Faraday cup placed inside the first dipole magnet of the Grand Raiden. The singly charged ^{3}He$^+$ ions which captured an electron from the target were also observed at the focal plane.

The tritons were detected by two multiwire drift chambers (MWDCs) [37] placed along the focal plane with an angle of 45° relative to the central ray of the spectrometer. Each MWDC consisted of two anode wire planes, with wires stretched in the vertical plane at an angle of 48.2° with respect to the vertical direction. Two ΔE plastic scintillator detectors were installed downstream from the MWDCs. They were used for particle identification and the generation of fast timing signals. A measured spectrum covered excitation energies up to about 25 MeV.

For good angle resolution in the vertical direction, the over-focus mode [28] of the Grand Raiden spectrometer was applied. In combination with angular dispersion matching, precise measurements of the scattering angles in both horizontal and vertical directions were realized. Owing to the good angle resolution, kinematic defocusing effects [26,27] in both directions were clearly observed and corrected for by software. The higher-order aberrations of the spectrometer were minimized by using multipole magnets and software corrections. As a

TABLE I. Correspondence of states observed in the present (p, p') measurement at 0°, (e, e'), and NRF studies, and the (p, p') measurement at finite angles. States above $E_x = 8$ MeV are shown.

Present (p, p')		(e, e)[a]		NRF[b]		(p, p')[c]
E_x (MeV)	$d\sigma/d\Omega$ (mb/sr)	E_x (MeV)	$B(M1)(\mu_N^2)$	E_x (MeV)	$B(M1)(\mu_N^2)$	E_x (MeV)
8.203	0.19(8)					
8.238	0.26(8)	8.240	1.27(20)	8.237[d]		
8.274	0.18(8)	8.276	0.26(3)			
8.372	0.16(8)					
8.419	0.17(8)					
8.461	0.19(8)			8.461	0.38(2)	
8.517	0.27(8)	8.516	1.04(15)	8.514[d]		
8.602	0.57(4)	8.601	0.44(5)	8.601	0.33(3)	
8.677	1.02(4)	8.680	0.47(3)	8.679	0.82(4)	
8.856	0.41(5)					
		8.817	0.19(2)			
8.880	0.19(5)	8.875	0.51(4)	8.880[d]		
8.959	0.32(4)	8.967	0.23(6)			
		9.037	0.30(4)			
9.071	0.35(4)	9.073	0.26(5)	9.073	0.31(2)	
9.156	0.36(4)	9.163	0.23(3)	9.157	0.20(3)	
9.193	0.18(4)			9.191[d]		
9.242	0.17(4)					
9.326	0.20(4)					
		9.368	0.34(4)	9.369[d]		
9.526	0.37(4)	9.513	0.22(15)	9.523[d]		
9.739	0.37(11)	9.755	0.32(5)			
9.835	0.33(4)	9.846[e]	0.54(7)			9.82
		10.073	0.35(3)			
10.115	0.22(4)	10.105	0.21(2)			
10.156	0.17(4)	10.157[e]	0.37(4)			
10.211	0.41(4)	10.218[e]	0.56(4)			10.18
		10.266	0.22(4)			
		10.355	0.24(3)			
		10.385	0.15(3)			
10.492	0.27(4)	10.514[e]	0.40(3)			10.48
		10.582	0.22(3)			
		10.633	0.32(12)			
10.664	1.59(5)	10.670[e]	1.25(6)			10.65
		10.806	0.12(4)			
		10.950	0.20(4)			
11.003	0.27(4)	11.013[e]	0.57(3)			10.98
		11.080	0.22(7)			
11.165	0.16(4)					
		11.265	0.11(2)			
11.672	0.31(9)	11.680	0.17(3)			
11.883	0.29(4)	11.860	0.4(3)			11.84
		11.990	0.32(6)			
12.197	0.23(4)					
12.293	0.21(4)					12.25
12.386	0.17(4)					
12.636	(0.12(4))					
12.738	0.32(4)					12.70
		12.796	0.47(9)			
		13.176	0.37(6)			
13.305	0.22(4)					13.25
		13.411	0.14(3)			
		13.716	0.30(2)			
		13.765	0.33(6)			

TABLE I. (*Continued.*)

Present (p, p')		(e, e)[a]		NRF[b]		(p, p')[c]
E_x (MeV)	$d\sigma/d\Omega$ (mb/sr)	E_x (MeV)	$B(M1)(\mu_N^2)$	E_x (MeV)	$B(M1)(\mu_N^2)$	E_x (MeV)
		14.081	0.22(5)			
		14.180	0.22(2)			
		14.852	0.20(4)			

[a]Reference [11].
[b]Reference [13].
[c]Reference [33].
[d]Assigned as $E1$ in Ref. [13].
[e]Identified as $T = 2$ in Ref. [11].

result, an energy resolution of 35 keV ($\Delta E/E = 8.3 \times 10^{-5}$) was achieved. A spectrum for scattering angles $0^\circ \leqslant \Theta \leqslant 0.8^\circ$ is shown in Fig. 5.

B. Data Analysis

The energy calibration along the focal plane of the spectrometer was done with the help of kinematic calculations using well-known discrete states observed in the (^{3}He,t) spectrum on a Mylar target (containing ^{12}C, ^{13}C, and ^{16}O). Calibration spectra were measured with the same magnet settings as used for the ^{58}Ni spectra. Owing to the small Q value of the (^{3}He,t) reaction on ^{13}C and the large Q values on ^{16}O and ^{12}C, the excitation energies in ^{58}Cu were determined by interpolation from the g.s. up to 11.5 MeV. We estimate that excitation energies up to this energy are accurate to within 10 keV.

Peaks in the spectra were fitted using the shape of the well-isolated 1.05 MeV state in ^{58}Cu as the standard. In Fig. 6, a typical example of the peak fitting analysis is shown. As can be seen from the spectrum in Fig. 5, an underlying continuum appears above 7 MeV. The proton separation energy S_p is 2.87 MeV. Therefore, this continuum is due to the three-body kinematics of the reaction and is called quasifree scattering. Since the theoretical shape of this continuum is not known at 0°, a smooth function was assumed connecting the minima in the spectrum. It is expected that the experimental background created by the beam was very small in the (^{3}He,t) spectra, because the strong magnetic field that is required to analyze tritons sweeps away other particles with a lower magnetic rigidity, including the $^3He^{2+}$ beam.

To examine the $L = 0$ nature, angular distributions of states within the acceptance of the Grand Raiden spectrometer were analyzed. Owing to the good angle resolution, angular distributions around 0° could be obtained. The precise 0° scattering angle was determined from the incident angle of singly charged $^3He^+$ particles in the focal plane that are produced by atomic-electron capture processes in the target. The relative decrease of the cross sections of each state at different scattering angle cuts was compared with that of the strongest GT state at 1.05 MeV. Below $E_x \approx 11$ MeV, most peaks showed similar forward-peaked angular distributions. It was found that the ratios of cross sections in the spectra with scattering angles of $\Theta \geqslant 1.4^\circ$ and $\Theta \leqslant 0.8^\circ$ for all observed 1^+ states had deviations within 15% compared with the ratio of the 1.05 MeV state, suggesting 0°-peaked angular distributions characteristic of $L = 0$ transfer. On the other hand, the ratios for excited states associated with $L \geqslant 1$ transfer ($\Delta J^\pi \neq 1^+$) were larger by more than 30%. All of these $L \geqslant 1$ states were weakly excited in the $\Theta \leqslant 0.8^\circ$ spectrum. At 3.54 MeV, an excited state with an angular distribution quite different from the adjacent GT states was found as shown in Fig. 7. The most prominent difference of strengths in the two angle cuts was observed for this state showing that the $L \geqslant 1$ contributions in the spectra are small in the 0° spectra. These facts are consistent

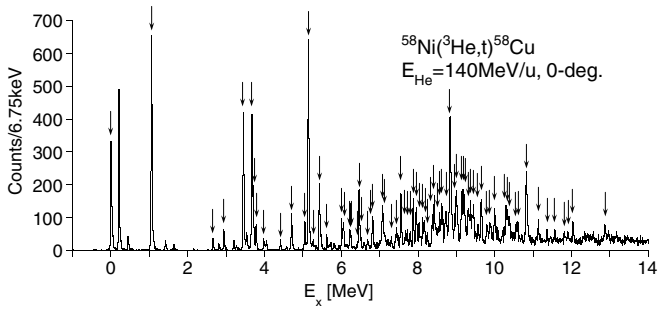

FIG. 5. Excitation energy spectrum of the ^{58}Ni(^{3}He,t) measurement. Events with scattering angles of $\sqrt{\theta^2 + \phi^2} \leqslant 0.8^\circ$ are shown. An energy resolution of 35 keV (FWHM) was achieved. GT states are indicated by vertical arrows.

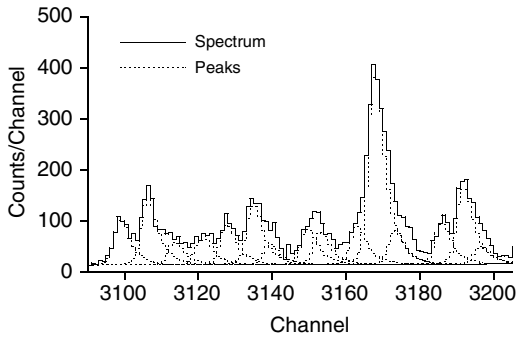

FIG. 6. Typical example of peak fitting analysis for the 8–9 MeV region of the (^{3}He,t) spectrum. Experimental spectrum (solid line) is decomposed into individual states by using the peak shape of a well-separated low-lying state as a peak-shape standard.

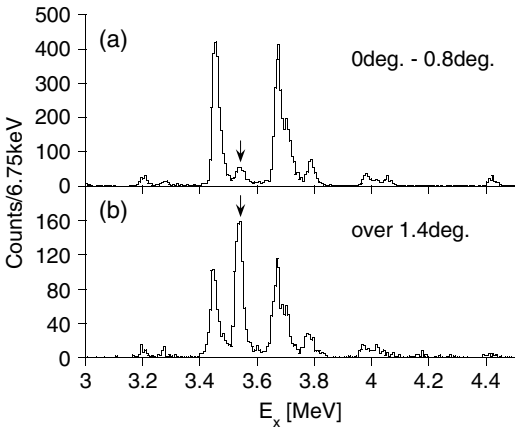

FIG. 7. (^{3}He,t) spectra in 3.0–4.5 MeV excitation energy region for scattering angles (a) 0°–0.8° and (b) $\geqslant$1.4° within the spectrometer acceptance. Angular distribution of the 3.54 MeV state is obviously different from the adjacent GT states.

with the result of the multipole decomposition analysis of the ^{58}Ni(p, n) spectrum, in which the $L \geqslant 1$ component is small below 10 MeV at 0° [15].

Since the kinematic and distortion factors in Eq. (2) change as functions of E_x and momentum transfer q, the unit cross section $\hat{\sigma}_{\rm GT}$ has to be corrected accordingly. In order to evaluate the E_x dependence of $\hat{\sigma}_{\rm GT}$, a DWBA calculation was performed for the (^{3}He,t) reaction by using the code DW81 [38] following the procedure discussed in Ref. [39]. We considered the configurations ($f_{5/2}$, $f_{7/2}^{-1}$), ($p_{3/2}$, $p_{3/2}^{-1}$), and ($p_{1/2}$, $p_{3/2}^{-1}$). A collective wave-function calculated by the code NORMOD was used. Optical potential parameters that were determined at an incident ^{3}He energy of 150 MeV/nucleon [40] were used. For the effective projectile-target interaction of the composite ^{3}He particle, the form derived by Schaeffer [41], with a strength of $V_{\sigma\tau} = -2.1$ MeV and a range $R = 1.415$ fm [42], was employed. For other details, see Ref. [12]. As a result, it was found that the unit cross section at 0° decreases gradually with excitation energy. It was about 10% lower at $E_x =$ 8 MeV and about 20% lower at $E_x = 12$ MeV relative to the g.s. Depending on the configuration used in the calculation, the amount of the decrease was different by a few percent. The errors on the transition strengths were determined from the ambiguities in the DWBA calculation and the peak fitting analysis. Although the effective strength of the tensor-τ term is not known well, the contribution was estimated roughly by the DWBA calculations. It is expected that the contribution is about 2% for the ($f_{5/2}$, $f_{7/2}^{-1}$) and ($p_{1/2}$, $p_{3/2}^{-1}$) configurations. A slightly larger contribution was estimated for the ($p_{3/2}$, $p_{3/2}^{-1}$) configuration. This configuration is expected to contribute mainly to the states in the lower excitation energy region.

The transition strengths obtained can be converted into B(GT) values by using Eq. (2) and the GT unit cross section $\hat{\sigma}_{\rm GT}$ that can be derived from the B(GT) value obtained in the β-decay study of ^{58}Cu [43,44], as was done in Ref. [12]. The determination of a more precise $\hat{\sigma}_{\rm GT}$ value not only from the β decay of ^{58}Cu but also from the β decay of ^{58}Zn to ^{58}Cu is in progress [45]. It is expected that the experiment will provide the strengths of GT transitions that are analogous to those discussed in the present paper up to an excitation energy of a few MeV. Because the main interest of this paper is the isospin structure of the $A = 58$ system above the 8 MeV region, the discussion is limited to using relative values.

V. ISOSPIN IDENTIFICATION

As discussed in Sec. II, isospin T_f of the final 1^+ states can be determined by comparing the strengths of analogous transitions in the CE and IE scattering reactions. In Ref. [12], the GT transition strengths to the states below $E_x = 8$ MeV in ^{58}Cu were derived with a resolution of 50 keV from the (^{3}He,t) spectrum. Isospin $T_f = 1$ was suggested for the states at 7.552, 7.869, and 8.026 MeV from a comparison of GT strengths with the analogous $M1$ transition strengths studied in a NRF measurement [13]. The improved energy resolution of 35 keV of the present (^{3}He,t) measurement allowed an analysis even for states at higher excitation energies where the level density is higher. In this section, by comparing the (^{3}He,t) data with the (p, p') data, the analogous structure, i.e., the isospin symmetry structure of $M1$ and GT states and the T_f distribution above 8 MeV is discussed. The comparison is extended to the results of GT$_+$ excitations, in which only $T_f = 2$ states are allowed.

A. Comparison between (p, p') and (^{3}He, t) data

In Fig. 8, the (p, p') and the (^{3}He,t) strengths can be compared in the excitation energy range from 8 to 14 MeV. The (^{3}He,t) spectrum is tentatively shifted by 0.16 MeV. With

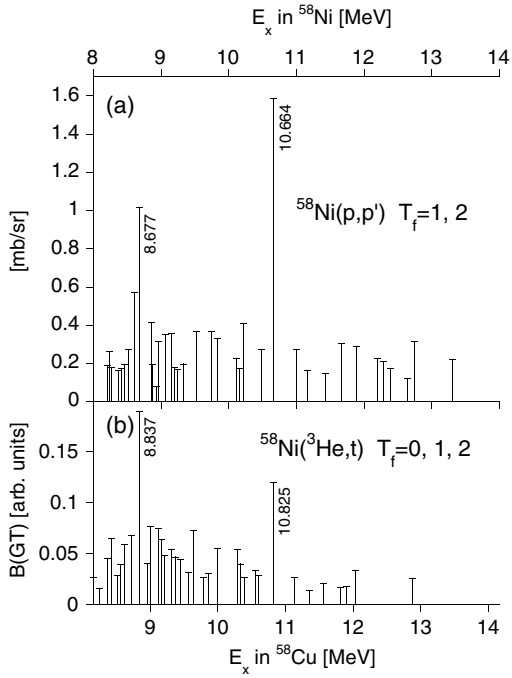

FIG. 8. (a) Cross sections of the (p, p') measurement from 8 to 14 MeV and (b) relative B(GT) strengths of the (^{3}He,t) measurement from 8.16 to 14.16 MeV. Vertical scale is normalized by the heights of the analog states at 8.677 MeV in the (p, p') reaction and at 8.837 MeV in the (^{3}He,t) reaction.

this energy shift, which is very close to the excitation energy of 0.203 MeV for the isobaric analog state (IAS) in ^{58}Cu, both strength distributions are very similar and the expected analogous structure of excited states can be seen. The vertical scales of the upper and lower panels of Fig. 8 are adjusted so that the 8.837 MeV state in the (^{3}He,t) reaction, the strongest $T_f = 1$ candidate state, has the same height as the 8.677 MeV state in the (p, p') reaction. In the discussion below, excitation energies in ^{58}Cu will be used to specify a pair of analog states with those in ^{58}Ni shown in parentheses.

A closer examination of the strength distributions of Fig. 8 shows that the relative strengths of analog excited states below and above 10 MeV are rather different. Compared with the states below 10 MeV, obviously the strength of analog states at 10.825(10.664) MeV is enhanced in the (p, p') spectrum (see Fig. 8) by nearly a factor of 3. As discussed in Sec. II B, the enhanced strength in the (p, p') spectrum suggests that this pair of analog states has $T_f = 2$. It is also suggested that states below 10 MeV are $T_f = 1$. This $T_f = 2$ assignment for the analog states at 10.825 (10.664) MeV is consistent with the report given in Ref. [11] by the (e, e') experiment (see Table I).

A ratio of 3 for $R_{\rm GT}$, which represents a ratio of CG coefficients, is expected for pairs of analog $T_f = 2$ states [see Eq. (5) for the definition of $R_{\rm GT}$]. Therefore, for the empirical determination of the ratios $R_{\rm GT}$ for pairs of analog states, we normalized the value of $R_{\rm GT}$ to 3 for the strongest pair of analog $T_f = 2$ states at 10.825 (10.664) MeV. The analogous relationship of the other states was determined from their excitation energies. Using the strong pairs at 8.837 (8.677) and 10.825 (10.664) MeV as the standard and assuming a linear relationship of the excitation energies of analogous pairs, states having the closest corresponding energies were treated as analog states.

Although the estimated contributions of the IS, tensor, and exchange terms to the proportionalities in the (p, p') and the (^{3}He,t) reactions are not negligibly small, the $T_f = 1$ and 2 states should be identified because the $R_{\rm GT}$ values are different by a factor of 3 for these states. The experimentally obtained $R_{\rm GT}$ values are summarized in Table II and Fig. 9.

The values of $R_{\rm GT}$ are clearly divided into two groups. Almost all pairs of analog states below 10 MeV show ratios of about 1, while those at higher energies show larger values. A typical example of the states below 10 MeV is the 8.837 (8.677) MeV state. It is the most strongly excited state in the (^{3}He,t) spectrum above 8 MeV. The $R_{\rm GT}$ value of 1.16 (13) is in good agreement with the value of unity expected for a $T_f = 1$ state. All pairs below 10 MeV show a ratio of less than 1.5 except for the pairs at 8.725 (8.602), 9.209 (9.071), and 9.861 (9.739) MeV. Since the lowest 1^+ state with $T = 2$ in ^{58}Co is at 1.049 MeV, we suggest that the lowest $T_f = 2$ analog states are at 9.861 (9.739) MeV. Although the 8.725 (8.602) and 9.209 (9.071) pairs have $R_{\rm GT}$ values larger than 1.5, they are identified to be $T_f = 1$. The larger values of $R_{\rm GT}$ can be due to the constructive contributions from the IS component and also the exchange term in the (p, p') reaction.

On the other hand, most pairs of analog states above 10 MeV show ratios larger than 1.5, typically 2.5. This is also in agreement with the value of 3 expected from the isospin CG coefficients. These results suggest that the states in the

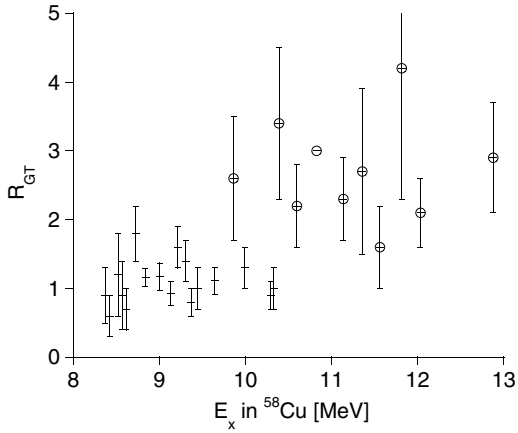

FIG. 9. Experimental ratios $R_{\rm GT}$ of analog states observed in the (^{3}He,t) and (p, p') measurements. From the isospin Clebsch-Gordan coefficients, expected $R_{\rm GT}$ values are 1 and 3 for $T_f = 1$ and 2 states, respectively. Candidates of $T_f = 2$ states are marked by open circles. Note that the $R_{\rm GT}$ value for the 10.825 MeV state has no error since this ratio was normalized to be 3.

first group are $T_f = 1$ and the second group are $T_f = 2$. This agrees with the repulsive nature of the isospin symmetry term of the nuclear interaction that pushes the $T_f = 2$ states to higher excitation energies compared to those for $T_f = 1$ states. The GT states in the (^{3}He,t) spectrum with no corresponding analog state were identified as $T_f = 0$. In Figs. 10(a) and 10(b) and Figs. 11(a) and 11(b), correspondence of analog states in the (^{3}He,t) and (p, p') measurements are shown for $T_f = 1$ and 2, respectively. Although the state at 9.526 MeV in ^{58}Ni is identified as $E1$ in Ref. [13], a candidate for analog state exists at 9.645 MeV in ^{58}Cu. The corresponding $R_{\rm GT}$ value of about 1 suggests that the pair of states has $J^\pi = 1^+$ and $T_f = 1$. A few excited states are observed in the (p, p') spectrum between 12.2 and 12.4 MeV, and corresponding weak states are also found in the (^{3}He,t) spectrum between 12.3 and 12.6 MeV.

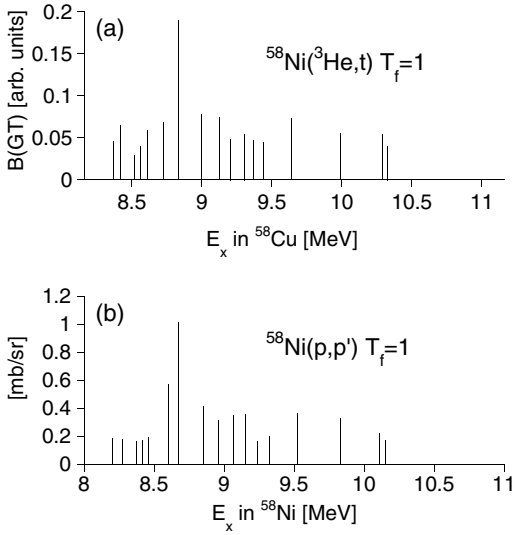

FIG. 10. Strength distributions of $T_f = 1$ states from (a) the (^{3}He,t) measurement and (b) (p, p') scattering.

TABLE II. Corresponding analog states observed in the (^{3}He,t) and (p, p') spectra and the R_{GT} values. The B(GT) values, cross sections, differences of excitation energies ΔE_x, and determined T_f values are shown. The B(GT) values in arbitrary units are given to show the relative strengths.

(^{3}He,t)		(p, p')		ΔE_x (MeV)	R_{GT}	T_f
E_x in ^{58}Cu (MeV)	B(GT) (a.u.)	E_x in ^{58}Ni (MeV)	Cross section (mb/sr)			
8.370	0.045(5)	8.203	0.19(8)	0.167	0.9(4)	1
8.421	0.065(6)	8.274	0.18(8)	0.147	0.6(3)	1
8.520	0.029(5)	8.372	0.16(8)	0.148	1.2(6)	1
8.566	0.039(5)	8.419	0.17(8)	0.147	0.9(5)	1
8.614	0.059(7)	8.461	0.19(8)	0.153	0.7(3)	1
8.725	0.068(11)	8.602	0.57(4)	0.123	1.8(4)	1
8.837	0.190(11)	8.677	1.02(4)	0.160	1.16(13)	1
8.959	0.040(5)					0
9.000	0.077(7)	8.856	0.41(5)	0.144	1.17(20)	1
9.129	0.075(6)	8.959	0.32(4)	0.170	0.93(17)	1
9.172	0.064(7)					0
9.209	0.048(6)	9.071	0.35(4)	0.138	1.6(3)	1
9.307	0.054(7)	9.156	0.36(4)	0.151	1.4(3)	1
9.371	0.047(6)	9.242	0.17(4)	0.129	0.8(2)	1
9.444	0.044(7)	9.326	0.20(4)	0.118	1.0(3)	1
9.567	0.032(5)					0
9.645	0.073(6)	9.526[a]	0.37(4)	0.119	1.11(19)	1
9.783	0.026(6)					0
9.861	0.031(6)	9.739[b]	0.37(11)	0.122	2.6(9)	2
9.989	0.055(6)	9.835[c]	0.33(4)	0.154	1.3(3)	1
10.291	0.054(6)	10.115	0.22(4)	0.176	0.9(2)	1
10.329	0.040(7)	10.156[c]	0.17(4)	0.173	1.0(3)	1
10.388	0.027(8)	10.211[b,c]	0.41(4)	0.177	3.4(1.1)	2
10.554	0.033(6)					0
10.597	0.028(6)	10.492[b,c]	0.27(4)	0.105	2.2(6)	2
10.825	0.120(8)	10.664[b,c]	1.59(5)	0.161	3.0[d]	2
11.137	0.027(5)	11.003[b,c]	0.27(4)	0.134	2.3(6)	2
11.358	(0.014(5))	11.165	0.16(4)	0.193	2.7(1.2)	2
11.562	(0.021(5))	11.423[b]	0.15(4)	0.139	1.6(6)	(2)
11.815	(0.017(5))	11.672[b]	0.31(9)	0.143	4.2(1.9)	2
11.903	(0.017(5))					0
12.034	0.033(6)	11.883[b]	0.29(4)	0.151	2.1(5)	2
		12.197[b]	0.23(4)			
12.3–12.6[e]		12.293[b]	0.21(4)			2
		12.386[b]	0.17(4)			
		12.636[b]	(0.12(4))			2
12.880	0.026(6)	12.738[b]	0.32(4)	0.142	2.9(8)	2
		13.305[b]	0.22(4)			

[a] Assigned as $E1$ state in Ref. [13].
[b] A corresponding state was found in the (d,^{2}He) spectrum [16].
[c] A corresponding state was observed in the (e, e') spectrum and identified to be $T = 2$ [11].
[d] R_{GT} value of 3.0 is given from the ratio of CG coefficients.
[e] Corresponding strengths were found in the (^{3}He,t) spectrum. For details, see text.

Even though we cannot determine R_{GT} values because of the lack of statistics, they are probably $T_f = 2$ states, because they are clearer and stronger in the (p, p') spectrum.

In the peak fitting procedure of the (^{3}He,t) spectrum, it was noticed that the results of the fit became better by assuming about 20% larger width for the states above 8 MeV excitation. It is suggested that there is a contribution from the proton decay to the widths of these states. In principle, proton decay from $T_f = 0$ and 1 states in ^{58}Cu leading to the g.s. of ^{57}Ni having $T = 1/2$ is possible above the proton separation energy of $S_p = 2.87$ MeV. On the other hand, the proton decay from $T_f = 2$ states to the same g.s. is not allowed by the isospin selection rule. The decay is possible only to the $T = 3/2$ excited states existing above $E_x = 5.14$ MeV. In order to decay to these $T = 3/2$ states, excitation energies above 8.01 MeV are required for the parent $T_f = 2$ states. As was discussed

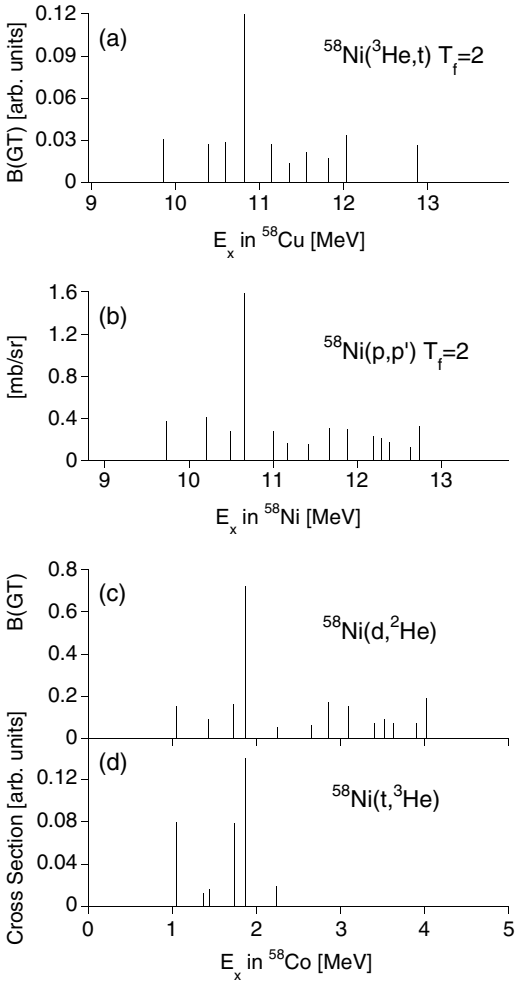

FIG. 11. Strength distributions of $T_f = 2, 1^+$ states obtained in the (a) (^{3}He,t), (b) (p, p'), (c) $(d,^2\text{He})$ [16], and (d) $(t,^3\text{He})$ [17] measurements. The $T_f = 2$ identification was performed using the ratio R_{GT}. For details, see text.

above, the first $T_f = 2$ GT state is observed at 9.861 MeV, which means that the proton decay channel is open also to all $T_f = 2$ states. Therefore, both $T_f = 1$ and 2 states can have a decay width. With a resolution of 35 keV, a large difference of the peak widths for the $T_f = 1$ and 2 states was not noticed.

In Fig. 12, the GT strength distributions are shown for $T_f = 0$, 1, and 2 states observed in the (^{3}He,t) spectrum. Since an excitation energy below 8 MeV could not be measured in the (p, p') spectrum, the results of the T_f identification given in Ref. [12] was adopted for the states in this region. As previously mentioned, the first attempt to decompose GT states in ^{58}Cu into different T_f was made using the ^{58}Ni(^{3}He,t) spectrum with an energy resolution of 140 keV. Although T_f distributions from both analyses are more or less in agreement, details are far better studied in the present analysis thanks to the improved energy resolution of 35 keV. In addition, the T_f identification in Ref. [10] was made by comparison with the (e, e') data [11]. This (e, e') data and the present (p, p') results for the identification of $M1$ states were not always consistent, as mentioned before.

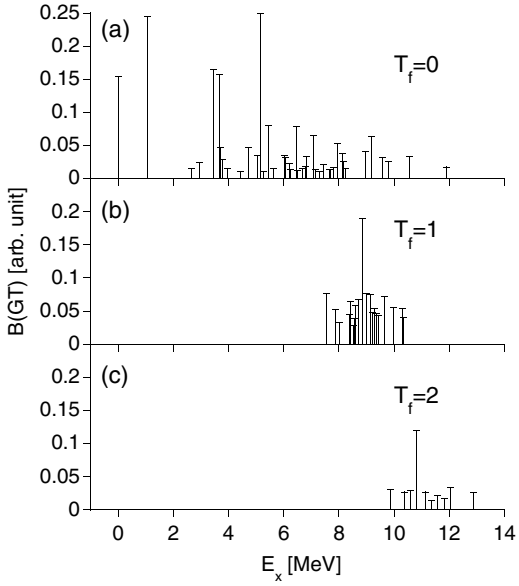

FIG. 12. B(GT) strength distribution in ^{58}Cu for $T_f = 0$, 1, and 2. Below 8 MeV, the T_f identification of Ref. [12] was adopted.

B. Comparison with (n, p)-type transitions

Since deuterons and the unbound g.s. of ^{2}He particles have J^π values of 1^+ and 0^+, respectively, the $(d,^2\text{He})$ reaction is a good probe to study GT$_+$ excitations. As shown in Fig. 1, GT$_+$ excitations from $T_i = 1$ nuclei lead only to $T_f = 2$ states. The GT$_+$ strength in ^{58}Co was studied in a ^{58}Ni$(d,^2\text{He})$ experiment at 0° performed at KVI, Groningen, using a 85 MeV/nucleon deuteron beam [16]. An energy resolution of 140 keV (FWHM) was achieved using the Big Bite magnetic spectrometer with a large acceptance [46]. In Ref. [17], using the ^{58}Ni$(t,^3\text{He})$ reaction at $E_t = 25$ MeV, $J^\pi = 1^+$ GT states in ^{58}Co were reported.

In Fig. 11, the strengths of $T_f = 2$ states identified in the (^{3}He,t) and (p, p') measurements can be compared with the reported 1^+ strengths measured in the $(d,^2\text{He})$ [16] and the $(t,^3\text{He})$ [17] experiments. The energy scales of the (^{3}He,t) and (p, p') strength distributions are shifted by the respective differences of 8.96 and 8.80 MeV relative to those of $(d,^2\text{He})$ and $(t,^3\text{He})$, respectively, so that the strongest $T_f = 2$ states align. A good correspondence of states between the (p, p') and (n, p)-type spectra was achieved by shifting the excitation energy by 8.80 MeV. This value agrees well with the excitation energy of 8.830 MeV for the IAS of the ^{58}Co g.s. in ^{58}Ni [47].

The $T_f = 2$ strengths in the (^{3}He,t), (p, p'), and $(d,^2\text{He})$ measurements show very good agreement not only in the excitation energies of the states but also in their relative strengths. In addition, states observed in the $(t,^3\text{He})$ spectrum show good correspondence in excitation energies. These facts confirm that the identification of T_f values by means of the ratio R_{GT} was successful. It should be noted that the incident energy of 25 MeV for the $(t,^3\text{He})$ measurement is too low to deduce precise B(GT) values.

By comparing the GT states observed in the $(t,^3\text{He})$ spectrum with $M1$ states observed by the ^{58}Ni(e, e') reaction, Mettner *et al.* [11] identified $T_f = 2$, $M1$ states in ^{58}Ni at

9.846, 10.157, 10.218, 10.514, 10.670, and 11.013 MeV. As indicated in Tables I and II, in our analysis using the R_{GT} value these states or very close neighboring states are assigned to be $T_f = 2$.

In Ref. [18], the B(GT) distribution of $T_f = 2$ strength is reported from the ^{58}Ni(n, p) measurement at 198 MeV. Their analysis showed that the GT strength distributes rather widely in the energy region up to 4 MeV in ^{58}Co. Our analysis also shows that the $T_f = 2$ GT strength is below 4 MeV, but the strength is concentrated around $E_x = 2$ MeV in ^{58}Co (see Fig. 11). Even if the poor resolution of the (n, p) reaction of ($\Delta E \approx 1$ MeV) is taken into account, the two distributions look rather different.

C. E_x differences of the analogous transitions

In Table II, differences of excitation energies ΔE_x of analog states in ^{58}Cu and ^{58}Ni are shown. To see more directly how the excitation energies of analog states correspond at higher excitations, we include the corrections of the E_x values of the IASs to the ΔE_x values. The IAS of the g.s. of ^{58}Ni is found at $E_x = 0.203$ MeV in ^{58}Cu. In addition, the IAS of the g.s. of ^{58}Co is found at $E_x = 8.830$ MeV in ^{58}Ni. Therefore, taking the E_x values of ^{58}Ni states as standards, the corrected ΔE_x values $\Delta E_{\rm corr}$ are defined as

$$\Delta E_{\rm corr} = \begin{cases} (E_{\rm Cu} - 0.203) - E_{\rm Ni}, \\ (E_{\rm Co} + 8.830) - E_{\rm Ni}, \end{cases}$$

where $E_{\rm Cu}$, $E_{\rm Ni}$, and $E_{\rm Co}$ are the E_x values of the corresponding excited analog states in ^{58}Cu, ^{58}Ni, and ^{58}Co, respectively. The $\Delta E_{\rm corr}$ values plotted in Fig. 13 as a function of the E_x values of the ^{58}Ni states are within the range of ± 100 keV, suggesting the good isospin symmetry in $A = 58$ isobars. However, the $\Delta E_{\rm corr}$ values for the ^{58}Cu-^{58}Ni pair are negative, while those for the ^{58}Co-^{58}Ni pair are positive. This suggests that at higher excitation energies, the Coulomb displacement energies become smaller in the higher-Z nucleus ^{58}Cu, while becoming larger in lower-Z nucleus ^{58}Co. No clear difference

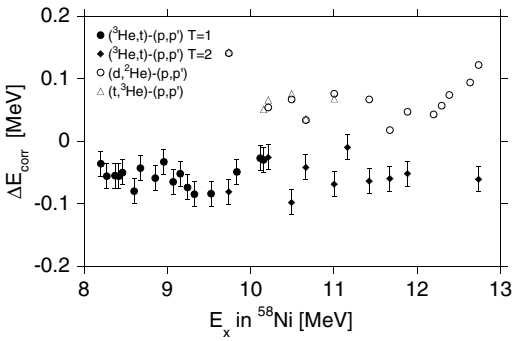

FIG. 13. Differences of the excitation energies $\Delta E_{\rm corr}$ between the excited states in the (p, p') spectrum and their analog states observed in the (^{3}He,t), (d,^{2}He), and (t,^{3}He) spectra. Solid circles and diamonds are for the analog states in the (^{3}He,t) spectrum having $T_f = 1$ and 2, respectively. Open circles and triangles are for the analog states in the (d,^{2}He) and (t,^{3}He) spectra, respectively. For details, see text.

in the $\Delta E_{\rm corr}$ values was found between the $T_f = 1$ and $T_f = 2$ states in the ^{58}Cu-^{58}Ni pair.

VI. SHELL-MODEL CALCULATIONS

Large-scale shell-model (SM) calculations are powerful tools for the theoretical evaluation of GT strength distributions. In astrophysics, SM calculations are important for the calculation of GT transitions starting even from unstable nuclei in the iron and nickel region, which in turn determine the stellar weak-interaction rates [3,4]. These rates have significant influence on the stellar evolution and nucleosynthesis and, in particular, the core collapse of massive stars that triggers a type II supernova explosion [48,49]. Therefore, a comparison between the experimental GT strength distribution and those of the SM calculations using modern shell-model interactions, such as FPD6 [50], KB3 [51], and GXPF1 [52], is of considerable interest.

The ^{58}Ni $\rightarrow$ ^{58}Cu GT$_-$ strength distributions have been calculated by Jokinen *et al.* [53] and by Caurier *et al.* [54] using FPD6 and KB3 interactions, respectively. SM calculations employing the KB3 interaction [51] have been found to give an excellent description of nuclei at the beginning of the *fp* shell ($A < 50$) [55]. However, Caurier *et al.* found that the original KB3 interaction gives a larger quasiparticle gap in the $N = Z = 28$ nucleus ^{56}Ni, which results in a relative underbinding of nuclei with N or Z larger than 28. Using a modified KB3 interaction, they could, in general, reproduce the experimental GT strength distributions well up to iron isotopes. The agreement, however, was less satisfactory for the nickel isotopes [54]. Calculated strengths are concentrated in the g.s. and the so-called GT resonance region centered at $E_x \approx 9.5$ MeV in ^{58}Cu. The strength distribution was not so well reproduced at lower excitation energies, where the configurations above the $N = Z = 28$ shell closure also take part.

To seek a better agreement for $A \geqslant 57$ nuclei, a recently developed KB3G interaction [56] was used. The calculations of Ref. [54] were extended to include 4p-4h correlations using the code NATHAN [57]. To look for finer detail of the structure observed in the present high energy resolution study, the calculated GT strength distribution was obtained after 150 Lanczos iterations for each final isospin. The results of the calculation are shown in Fig. 14 together with the empirical B(GT) distribution. The usual "quenching factor" of $(0.74)^2$ [58] was applied.

The $T_f = 0$ GT strength distribution is now better reproduced except for a few states around 3.5 MeV.[1] The strong $T_f = 0$ state at 5.143 MeV seems to be more fragmented in the calculation. It is expected that going beyond 4p-4h correlations will produce a further fragmentation of the theoretical low-lying peaks resulting in better agreement with the experiment.

As shown in Fig. 12, fragmentation of the $T_f = 1$ and 2 GT strengths around the strongest state was observed.

[1]Corresponding structure is found in the calculation applying the GXPF1 interaction [59].

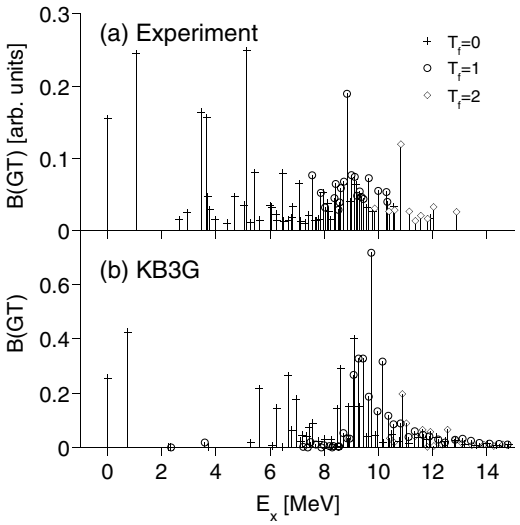

FIG. 14. Comparison between (a) experimentally obtained B(GT) values and (b) those from shell-model calculations applying the KB3G interaction. For details of the calculation, see text. Empirical B(GT) values in (a) are in arbitrary units.

Similar structure was obtained by the SM calculation (see Fig. 14). In particular for the $T_f = 2$ strengths, the location of the strongest state and the strength distribution are well reproduced. In the (^{3}He,t) spectrum, the strongest $T_f = 2$ state was observed at 10.825 MeV, while in the SM calculation it is at 10.876 MeV. In a simple single-particle picture, the expected main configuration of the $T_f = 2$ states is $(f_{7/2}^{-1}, f_{5/2})$. It is suggested that the good description of the excitation energies of the $T_f = 2$ states results from the $(f_{7/2}^{-1}, f_{5/2})$ configuration alone describing the $T_f = 2$ states. Note that the KB3 interaction generally reproduces well the structure of f-shell nuclei. The calculated $T_f = 0$, 1, and 2 strengths are 48%, 43%, and 9% of the total strength, respectively. On the other hand, obtained $T_f = 0$, 1, and 2 strengths are 57%, 34%, and 9%, respectively, in the (^{3}He,t) measurement.

VII. SUMMARY

The ^{58}Ni(^{3}He,t) experiment was performed at an incident beam energy of 140 MeV/nucleon using the Grand Raiden magnetic spectrometer. By applying the dispersion matching techniques to the system consisting of the WS beamline and the Grand Raiden magnetic spectrometer, an energy resolution of 35 keV ($\Delta E/E = 8.3 \times 10^{-5}$) was achieved. This resolution is one order of magnitude better than that in comparable ^{58}Ni(p, n) measurements at intermediate energies. Therefore, we could observe discrete states up to $E_x = 13$ MeV in ^{58}Cu. In the excitation energy region from 8 to 10 MeV, 1^+ states could be identified on average about every 50 keV. The horizontal and vertical components of the scattering angle were determined accurately by applying angular dispersion matching and the over-focus mode of the spectrometer, respectively.

The ^{58}Ni(p, p') experiment was performed with an incident beam energy of 160 MeV at IUCF using the K600 magnetic spectrometer. In proton inelastic scattering at 0°, correspondence with the (^{3}He,t) experiment is expected except for a contribution from the isoscalar term. Spectra were obtained in the ^{58}Ni(p, p') experiment at 0° even though such inelastic scattering measurements are very difficult. Discrete states were observed above $E_x = 8$ up to 14 MeV. Good energy resolution of 35 keV ($\Delta E/E = 2.2 \times 10^{-4}$) and good angle resolution were achieved.

The isospin symmetry structure of excited states in ^{58}Ni and ^{58}Cu was investigated by comparing the (p, p') and (^{3}He,t) spectra in the $E_x = 8$–14 MeV region. In these spectra, analog 1^+ states having isospin $T_f = 1$ and 2 should be commonly observed, while $T_f = 0$ states should exist only in the (^{3}He,t) spectrum. Many pairs of analog states were found at corresponding excitation energies in the (p, p') and (^{3}He,t) spectra. According to the isospin CG coefficients for the $T_i = 1$ system, the ratio of the excitation strengths $R_{\rm GT}$ has a value of 3 for pairs of $T_f = 2$ analog states and unity for the $T_f = 1$ states. Thus, from the ratio $R_{\rm GT}$, T_f values were identified for the pairs of analog states. The $T_f = 2$ strength distribution was further compared with that from the ^{58}Ni(d,^{2}He), ^{58}Ni(t,^{3}He), and ^{58}Ni(n, p) measurements. There was good agreement between the $T_f = 2$ distributions in our results and those for (d,^{2}He) scattering. The excitation energies of the $T_f = 2$ states from the (t,^{3}He) investigation also showed good agreement with our results.

ACKNOWLEDGMENTS

The ^{58}Ni(p, p') experiment was performed at IUCF as a part of experiment E409. We would like to express our gratitude to the accelerator group of IUCF, especially to Dr. G. East, for their effort in providing a high-quality halo-free proton beam. The ^{58}Ni(^{3}He,t)^{58}Cu experiment was performed at RCNP as part of the experiments E113 and E158. We are grateful to the RCNP accelerator group, especially to Prof. T. Saito and Dr. S. Ninomiya, for their effort in providing a high-quality ^{3}He beam indispensable for the realization of the matching conditions. Also, H.F. thanks Prof. J. Carter (University of the Witwatersrand, Johannesburg) for his comments.

[1] F. Osterfeld, Rev. Mod. Phys. **64**, 491 (1992), and references therein.

[2] J. Rapaport and E. Sugarbaker, Annu. Rev. Nucl. Part. Sci. **44**, 109 (1994).

[3] G. M. Fuller, W. A. Fowler, and M. J. Newman, Astrophys. J. Suppl. Ser. **42**, 447 (1980); **48**, 279 (1982) ; Astrophys. J. **252**, 715 (1982).

[4] K. Langanke and G. Martínez-Pinedo, Rev. Mod. Phys. **75**, 819 (2003).

[5] T. N. Taddeucci, C. A. Goulding, T. A. Carey, R. C. Byrd, C. D. Goodman, C. Gaarde, J. Larsen, D. J. Horen, J. Rapaport, and E. Sugarbaker, Nucl. Phys. **A469**, 125 (1987), and references therein.

[6] B. D. Anderson, T. Chittrakarn, A. R. Baldwin, C. Lebo,

R. Madey, P. C. Tandy, J. W. Watson, C. C. Foster, B. A. Brown, and B. H. Wildenthal, Phys. Rev. C **36**, 2195 (1987).
[7] Y. Fujita, H. Akimune, I. Daito, H. Fujimura, M. Fujiwara, M. N. Harakeh, T. Inomata, J. Jänecke, K. Katori, A. Tamii, M. Tanaka, H. Ueno, and M. Yosoi, Phys. Rev. C **59**, 90 (1999).
[8] Y. Fujita, B. A. Brown, H. Ejiri, K. Katori, S. Mizutori, and H. Ueno, Phys. Rev. C **62**, 044314 (2000), and references therein.
[9] Y. Fujita, Y. Shimbara, I. Hamamoto, T. Adachi, G. P. A. Berg, H. Fujimura, H. Fujita, J. Görres, K. Hara, K. Hatanaka, J. Kamiya, T. Kawabata, Y. Kitamura, Y. Shimizu, M. Uchida, H. P. Yoshida, M. Yoshifuku, and M. Yosoi, Phys. Rev. C **66**, 044313 (2002).
[10] Y. Fujita, H. Akimune, I. Daito, M. Fujiwara, M. N. Harakeh, T. Inomata, J. Jänecke, K. Katori, H. Nakada, S. Nakayama, A. Tamii, M. Tanaka, H. Toyokawa, and M. Yosoi, Phys. Lett. **B365**, 29 (1996).
[11] W. Mettner, A. Richter, W. Stock, B. C. Metsch, and A. G. M. van Hees, Nucl. Phys. **A473**, 160 (1987).
[12] Y. Fujita, H. Fujita, T. Adachi, G. P. A. Berg, E. Caurier, H. Fujimura, K. Hara, K. Hatanaka, Z. Janas, J. Kamiya, T. Kawabata, K. Langanke, G. Martínez-Pinedo, T. Noro, E. Roeckl, Y. Shimbara, T. Shinada, S. Y. van der Werf, M. Yoshifuku, M. Yosoi, and R. G. T. Zegers, Eur. Phys. J. A **13**, 411 (2002).
[13] F. Bauwens, J. Bryssinck, D. De Frenne, K. Govaert, L. Govor, M. Hagemann, J. Heyse, E. Jacobs, W. Mondelaers, and V. Yu. Ponomarev, Phys. Rev. C **62**, 024302 (2000).
[14] K. Hara, T. Adachi, H. Akimune, I. Daito, H. Fujimura, Y. Fujita, M. Fujiwara, K. Fushimi, K. Y. Hara, M. N. Harakeh, K. Ichihara, T. Ishikawa, J. Jänecke, J. Kamiya, T. Kawabata, K. Kawase, K. Nakanishi, Y. Sakemi, Y. Shimbara, Y. Shimizu, M. Uchida, H. P. Yoshida, M. Yosoi, and R. G. T. Zegers, Phys. Rev. C **68**, 064612 (2003).
[15] J. Rapaport, T. Taddeucci, T. P. Welch, C. Gaarde, J. Larsen, D. J. Horen, E. Sugarbaker, P. Koncz, C. C. Foster, C. D. Goodman, C. A. Goulding, and T. Masterson, Nucl. Phys. **A410**, 371 (1983).
[16] M. Hagemann, A. M. van den Berg, D. De Frenne, V. M. Hannen, M. N. Harakeh, J. Heyse, M. A. de Huu, E. Jacobs, K. Langanke, G. Martínez-Pinedo, and H. J. Wörtche, Phys. Lett. **B579**, 251 (2004); M. Hagemann, C. Bäumer, A. M. van den Berg, D. De Frenne, D. Frekers, V. M. Hannen, M. N. Harakeh, J. Heyse, M. A. de Huu, E. Jacobs, K. Langanke, G. Martínez-Pinedo, A. Negret, L. Popescu, S. Rakers, R. Schmidt, and H. J. Wörtche, Phys. Rev. C **71**, 014606 (2005).
[17] F. Ajzenberg-Selove, Ronald E. Brown, E. R. Flynn, and J. W. Sunier, Phys. Rev. C **31**, 777 (1985); F. Ajzenberg-Selove, Ronald E. Brown, E. R. Flynn, and J. W. Sunier, Phys. Rev. C **30**, 1850 (1984).
[18] S. El-Kateb, K. P. Jackson, W. P. Alford, R. Abegg, R. E. Azuma, B. A. Brown, A. Celler, D. Frekers, O. Häusser, R. Helmer, R. S. Henderson, K. H. Hicks, R. Jeppesen, J. D. King, K. Raywood, G. G. Shute, B. M. Spicer, A. Trudel, M. Vetterli, and S. Yen, Phys. Rev. C **49**, 3128 (1994).
[19] A. R. Edmonds, *Angular Momentum in Quantum Mechanics* (Princeton University, Princeton, NJ, 1960).
[20] W. G. Love and M. A. Franey, Phys. Rev. C **24**, 1073 (1981); M. A. Franey and W. G. Love, Phys. Rev. C **31**, 488 (1985).
[21] Y. Fujita, Y. Shimbara, T. Adachi, G. P. A. Berg, B. A. Brown, H. Fujita, K. Hatanaka, J. Kamiya, K. Nakanishi, Y. Sakemi, S. Sasaki, Y. Shimizu, Y. Tameshige, M. Uchida, T. Wakasa, and M. Yosoi, Phys. Rev. C **70**, 054311 (2004).
[22] Y. Shimbara, Ph.D. thesis, Osaka University, 2005.
[23] J. W. Watson, W. Pairsuwan, B. D. Anderson, A. R. Baldwin, B. S. Flanders, R. Madey, R. J. McCarthy, B. A. Brown, B. H. Wildenthal, and C. C. Foster, Phys. Rev. Lett. **55**, 1369 (1985).
[24] G. P. A. Berg, L. C. Bland, B. M. Cox, D. DuPlantis, D. W. Miller, K. Murphy, P. Schwandt, K. A. Solberg, E. J. Stephenson, B. Flanders, and IUCF Sci. Tech. Rep. 1986–1987 (unpublished), p.152.
[25] C. C. Foster and G. P. A. Berg, IUCF Sci. Tech. Rep.1988–1989 (unpublished), p.193.
[26] H. Fujita, Y. Fujita, G. P. A. Berg, A. D. Bacher, C. C. Foster, K. Hara, K. Hatanaka, T. Kawabata, T. Noro, H. Sakaguchi, Y. Shimbara, T. Shinada, E. J. Stephenson, H. Ueno, and M. Yosoi, Nucl. Instrum. Methods Phys. Res. A **484**, 17 (2002).
[27] Y. Fujita, K. Hatanaka, G. P. A. Berg, K. Hosono, N. Matsuoka, S. Morinobu, T. Noro, M. Sato, K. Tamura, and H. Ueno, Nucl. Instrum. Methods Phys. Res. B **126**, 274 (1997).
[28] H. Fujita, G. P. A. Berg, Y. Fujita, K. Hatanaka, T. Noro, E. J. Stephenson, C. C. Foster, H. Sakaguchi, M. Itoh, T. Taki, K. Tamura, and H. Ueno, Nucl. Instrum. Methods Phys. Res. A **469**, 55 (2001).
[29] S. C. Fultz, R. A. Alvarez, B. L. Berman, and P. Meyer, Phys. Rev. C **10**, 608 (1974).
[30] F. Ajzenberg-Selove, Nucl. Phys. **A506**, 1 (1990); **A523**, 1 (1990); D. R. Tilley, H. R. Weller, C. M. Cheves, Nucl. Phys. **A564**, 1 (1993); P. M. Endt, Nucl. Phys. **A521**, 1 (1990); **A633**, 1 (1998).
[31] J. Raynal, computer code DWBA98, NEA 1209/05 (1999).
[32] P. Schwandt, H. O. Meyer, W. W. Jacobs, A. D. Bacher, S. E. Vigdor, M. D. Kaitchuck, and T. R. Donoghue, Phys. Rev. C **26**, 55 (1982).
[33] C. Djalali, N. Marty, M. Morlet, A. Willis, J. C. Jourdain, N. Anantaraman, G. M. Crawley, A. Galonsky, and P. Kitching, Nucl. Phys. **A388**, 1 (1982); N. Marty, C. Djalali, M. Morlet, A. Willis, J. C. Jourdain, N. Anantaraman, G. M. Crawley, and A. Galonsky, *ibid*. **A396**, 145c (1983).
[34] I. Miura *et al*., RCNP Annual Rep. 1991 (unpublished), p.149.
[35] T. Wakasa, K. Hatanaka, Y. Fujita, G. P. A. Berg, H. Fujimura, H. Fujita, M. Itoh, J. Kamiya, T. Kawabata, K. Nagayama, T. Noro, H. Sakaguchi, Y. Shimbara, H. Takeda, K. Tamura, H. Ueno, M. Uchida, M. Uraki, and M. Yosoi, Nucl. Instrum. Methods Phys. Res. A **482**, 79 (2002).
[36] M. Fujiwara, H. Akimune, I. Daito, H. Fujimura, Y. Fujita, K. Hatanaka, H. Ikegami, I. Katayama, K. Nagayama, N. Matsuoka, S. Morinobu, T. Noro, M. Yoshimura, H. Sakaguchi, Y. Sakemi, A. Tamii, and M. Yosoi, Nucl. Instrum. Methods Phys. Res. A **422**, 484 (1999).
[37] T. Noro *et al*., RCNP Annual Rep. 1991 (unpublished), p. 177.
[38] DW81, a DWBA computer code by J. R. Comfort (1981), an extended version of DWBA70 by R. Schaeffer and J. Raynal (1971).
[39] S. van der Werf, S. Brandenburg, P. Grasdijk, W. A. Sterrenburg, M. N. Harakeh, M. B. Greenfield, B. A. Brown, and M. Fujiwara, Nucl. Phys. **A496**, 305 (1989).
[40] T. Yamagata, H. Utsunomiya, M. Tanaka, S. Nakayama, N. Koori, A. Tamii, Y. Fujita, K. Katori, M. Inoue, M. Fujiwara, and H. Ogata, Nucl. Phys. **A589**, 425 (1995).
[41] R. Schaeffer, Nucl. Phys. **A164**, 145 (1971).

[42] R. G. T. Zegers, H. Abend, H. Akimune, A. M. van den Berg, H. Fujimura, H. Fujita, Y. Fujita, M. Fujiwara, S. Galés, K. Hara, M. N. Harakeh, T. Ishikawa, T. Kawabata, K. Kawase, T. Mibe, K. Nakanishi, S. Nakayama, H. Toyokawa, M. Uchida, T. Yamagata, K. Yamasaki, and M. Yosoi, Phys. Rev. Lett. **90**, 202501 (2003).

[43] Z. Janas, M. Karny, Y. Fujita, L. Batist, D. Cano-Ott, R. Collatz, P. Dendooven, A. Gadea, M. Gierlik, M. Hellström, Z. Hu, A. Jokinen, R. Kirchner, O. Klepper, F. Moroz, M. Oinonen, H. Penttilä, A. Plochocki, E. Roeckl, B. Rubio, M. Shibata, J. L. Tain, and V. Wittman, Eur. Phys. J. A **12**, 143 (2001).

[44] K. Peräjärvi, P. Dendooven, M. Górska, J. Huikari, A. Jokinen, V. S. Kolhinen, M. La Commara, G. Lhersonneau, A. Nieminen, S. Nummela, H. Penttilä, E. Roeckl, J. C. Wang, and J. Äystö, Nucl. Phys. **A696**, 233 (2001).

[45] A. Kankainen (Univ. of Jyväskylä, private communication).

[46] A. M. van den Berg, Nucl. Instrum. Methods Phys. Res. B **99**, 637 (1995).

[47] M. R. Bhat, Nucl. Data Sheets **80**, 789 (1997).

[48] K. Langanke and G. Martínez-Pinedo, Nucl. Phys. **A673**, 481 (2000).

[49] A. Heger, K. Langanke, G. Martínez-Pinedo, and S. E. Woosley, Phys. Rev. Lett. **86**, 1678 (2001).

[50] W. A. Richter, M. G. van der Merwe, R. E. Julies, and B. A. Brown, Nucl. Phys. **A523**, 325 (1991); Nucl. Phys. **A577**, 585 (1994).

[51] A. Poves and A. P. Zuker, Phys. Rep. **70**, 235 (1981).

[52] M. Honma, T. Otsuka, B. A. Brown, and T. Mizusaki, Phys. Rev. C **69**, 034335 (2004).

[53] A. Jokinen, M. Oinonen, J. Äystö, P. Baumann, P. Dendooven, F. Didierjean, V. Fedoseyev, A. Huck, Y. Jading, A. Knipper, M. Koizumi, U. Köster, J. Lettry, P. O. Lips, W. Liu, V. Mishin, M. Ramdhane, H. Ravn, E. Roeckl, V. Sebastian, G. Walter, and ISOLDE Collaboration, Eur. Phys. J. A **3**, 271 (1998); and private communication.

[54] E. Caurier, K. Langanke, G. Martínez-Pinedo, and F. Nowacki, Nucl. Phys. **A653**, 439 (1999), and references therein.

[55] E. Caurier, A. P. Zuker, A. Poves, and G. Martínez-Pinedo, Phys. Rev. C **50**, 225 (1994).

[56] A. Poves, J. Sanchez-Solano, E. Caurier, and F. Nowacki, Nucl. Phys. **A694**, 157 (2001).

[57] E. Caurier, G. Martínez-Pinedo, F. Nowacki, A. Poves, J. Retamosa, and A. P. Zuker, Phys. Rev. C **59**, 2033 (1999).

[58] G. Martínez-Pinedo, A. Poves, E. Caurier, and A. P. Zuker, Phys. Rev. C **53**, R2602 (1996).

[59] M. Honma (private communication).